ELSEVIER

Earth and Planetary Science Letters 128 (1994) 37–46

EPSL

Changes in the lithospheric structure across the Sorgenfrei–Tornquist Zone inferred from dispersion of Rayleigh waves

H.A. Pedersen [a], M. Campillo [a], N. Balling [b]

[a] *Laboratoire de Géophysique Interne et Tectonophysique, Université Joseph Fourier, BP 53 ×, 38041 Grenoble Cedex, France*
[b] *Department of Earth Sciences, Geophysical Laboratory, University of Aarhus, Finlandsgade 6, 8200 Aarhus N, Denmark*

Received 11 April 1994; accepted 4 July 1994

Abstract

Surface wave analysis was used to study possible lateral changes in the lithospheric/upper mantle structure across the Sorgenfrei–Tornquist Zone (STZ), which is part of the transition zone between the ancient Baltic Shield and younger western Europe. Records of long period surface waves from earthquakes at teleseismic distances were analysed. The data originated from long period permanent stations in southeastern Norway and from broadband NARS stations installed in Denmark between 1983 and 1986. This configuration made it possible to compare the lithospheric structure north and south of the STZ by analysis of surface wave dispersion between pairs of closely spaced stations in the same tectonic unit. Phase velocities of fundamental mode Rayleigh waves were determined by calculating cross spectra of pairs of records.

The phase velocity dispersion curves show significant differences between the two tectonic units north and south of STZ. Linearized inversion of the observed dispersion curves, to obtain models of shear wave velocity in the crust and upper mantle, shows a low velocity zone (LVZ) at a depth of about 110 km beneath the western part of Denmark, just south of the STZ. A similar LVZ was not identified beneath southeastern Norway, north of the STZ. If a low velocity zone is present beneath the Baltic Shield in this area it must be very weak. The lateral changes in lithospheric–asthenospheric structures take place over a distance of less than 500 km. Our results therefore suggest that the STZ coincides with a transition zone in the upper mantle.

1. Introduction

The Tornquist Zone (TZ) is one of the most prominent tectonic lineaments across Europe. The TZ separates the Baltic shield and the East European Platform from the significantly younger Phanerozoic terranes and mobile belts of central and western Europe. The TZ is associated with significant lateral variations in geophysical and geotectonic characteristics. From the shield and platform to the tectonically younger areas, the crustal thickness decreases [1,2], heat-flow density generally increases [3–6] and the shear wave velocity structure of the uppermost mantle changes significantly [7–15].

The TZ in southern Scandinavia has a particularly complicated history and its tectonic significance is still debated. It seems to split into at least two main branches: a northern one, the Sorgenfrei–Tornquist Zone (STZ)/Fennoscan-

SSDI 0012-821X(94)00171-5

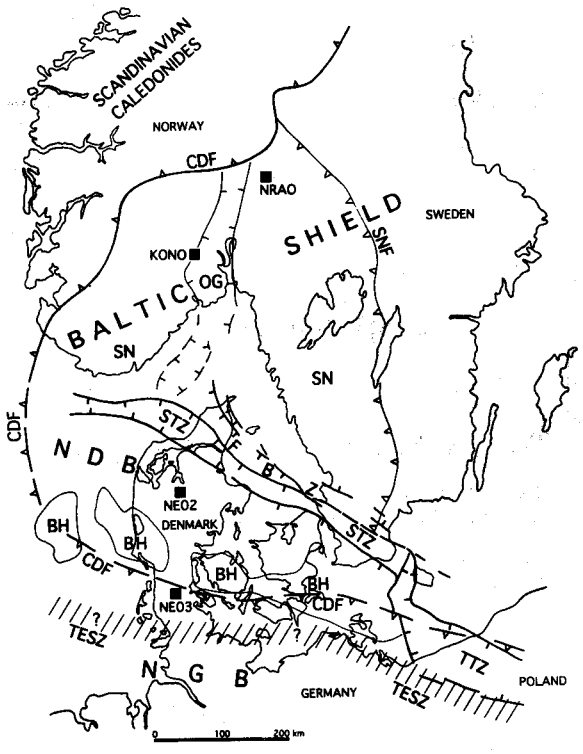

Fig. 1. Main tectonic units along the southwestern boundary of the Baltic Shield. *SN* = Sveconorwegian province; *SNF* = Sveconorwegian front; *CDF* = Caledonian deformation front; *FBZ* = Fennoscandian Border Zone; *STZ* = Sorgenfrei–Tornquist Zone; *TTZ* = Teisseyre–Tornquist Zone; *NDB* = Norwegian–Danish Basin; *BH* = basement highs; *NGB* = North German Basin; *TESZ* = element of Trans-European Suture Zone (inferred); *OG* = Oslo Graben. Mainly after [17]. Positions of seismological stations (NRA0, KONO, NE02 and NE03) used in this study are indicated by squares.

dian Border Zone (FBZ), and a southern one, located south of the Ringkøbing–Fyn basement high in Denmark (cf. Fig. 1). For a discussion of the tectonic history of the TZ in this area, see [16,17].

Various studies have confirmed the existence of significant lateral velocity variations in the uppermost mantle beneath southern Scandinavia [9,14,18]. Previous surface wave studies have focused on lateral variations on a regional scale. Calcagnile [9] studied long period Rayleigh waves propagating between distant seismological stations in Scandinavia to obtain a model of shear wave velocities in the uppermost mantle. He showed that the structure of the mantle varies significantly in the shield, with a thickening of the seismic lithosphere towards the central and northern parts of the shield. This thickening is combined with a weakening of an LVZ present below the lithosphere in the area. In a later study [14], Calcagnile pointed out differences in mantle structure between a profile running S–N and another profile which was located in southeastern Scandinavia. The differences persisted down to a depth of approximately 350 km. Stuart [19] studied Rayleigh wave dispersion across the North Sea. He suggested the presence of an LVZ from a depth of approximately 100 km in this area.

South of Denmark, both surface wave and long period body waves have been used to estimate shear waves in the upper mantle, based on data from the NARS array (1983–1987 configuration). Dost [13,20] found an average model along the array with an LVZ from a depth of 140 km and suggested that no LVZ was present beneath southern Scandinavia. Nolet [21] studied lateral heterogeneities along the array and found the northern limit of the LVZ to be located beneath the Paris Basin. Snieder [11] and Zielhuis and Nolet [15] suggested models of shear wave velocities in the upper mantle for which the eastern part of the Tornquist Zone is associated with significant anomalies of shear wave velocities in the upper mantle. For these studies the exact location of the shield–platform transition is not well resolved in the Danish area. Other surface wave studies in central and northern Europe (e.g., [10,12]) do not have sufficient station coverage to resolve details of the mantle structures in southern Scandinavia.

In this paper we study the shield–platform transition in southern Scandinavia by analysis of Rayleigh waves recorded at two pairs of closely spaced stations north of the STZ (southeastern Norway) and south of the STZ (western Denmark). The four stations are shown in Fig. 1. Two of them are broad-band NARS stations (NE02 and NE03), installed in Denmark between 1983 and 1986. The two stations in Norway are permanent stations: NRA0 is part of the NORESS array north of Oslo and KONO is a WWSSN station located south west of Oslo. The Oslo

Graben, a Permian structure, is located between the two stations in Norway. Previous studies have shown, however, that the Oslo Graben has played a minor role in the thermal and tectonic evolution of the transition zone and there is no indication that it affects the structure of the upper mantle (for a review see, e.g., [16]). Furthermore, surface waves are influenced by the shear wave structure over a large region around the direct path, so a weak anomaly in mantle structure beneath the Oslo Graben can probably not be resolved by analysis of surface wave dispersion. In this paper we characterize separately the dispersion curves for western Denmark (profile NE02–NE03) and southern Norway (profile NRA0–KONO) to study whether the STZ coincides with a major change in upper mantle structure.

2. Data selection

For each pair of stations, records of long period Rayleigh waves were retrieved from published data on CD-rom (NE02 and NE03: ORFEUS Data Center; NRA0 and KONO: USGS-NEIC). NORSAR provided us with supplementary data.

For phase velocity calculations it is necessary to use records of earthquakes for which a great circle passes approximately through the hypocenter and the two stations. For events that fulfilled this criteria, the signal to noise ratio as a function of frequency was calculated for each record. A multiple filter analysis was performed on each record [22] to obtain the group velocities. In this way it was possible to estimate whether the Rayleigh wave was well separated from other seismic phases. Such separation is essential for the phase velocity analysis because, when the distance between the two stations is small, seismic phases that arrive at the same time as the Rayleigh wave can be present on both records and may introduce systematic errors in the phase velocity measurements. Furthermore, the group velocities calculated at the two stations are expected to be very similar for the same event because the distance between stations is much smaller than the epicentral distance. The local structure between the stations, in this case, does not influence the group velocities significantly.

Very few events passed the selection procedure. Only records of 2 events were retained for the profile between the two NARS stations in Denmark. These 2 pairs of records are, at present, the only data available locally for the Danish area. For the two long period stations, KONO and NRA0, in southeastern Norway, a larger number of records were retained. We chose the 9 pairs of records which seemed to be of highest quality. Table 1 shows characteristics of the 11 events and Table 2 gives epicentral distances of the events and theoretical arrival angles relative

Table 1
Characteristics of events for which Rayleigh waves have been analysed

Date	Origin time	Latitude	Longitude	Depth (km)	Mb	Ms
840211	08:02:50.5	38.4N	22.1E	19	5.3	5.5
850606	02:40:12.9	0.9N	28.4W	10	6.3	6.5
851012	22:20:37.6	0.8N	29.9W	10	5.3	6.0
851018	03:22:23.2	37.5N	136.9E	33	5.8	4.9
860212	02:59:31.8	36.4N	140.9E	44	6.0	5.8
860515	06:38:37.7	52.3N	174.7W	33	5.6	6.4
860517	16:20:22.8	52.3N	174.6W	33	5.7	6.6
861122	00:41:43.1	34.4N	139.5E	10	5.9	5.7
861130	20:15:32.8	38.9N	142.0E	56	5.9	5.9
870206a	12:23:48.3	37.0N	141.7E	37	5.9	6.3
870206b	13:16:17.6	37.0N	141.7E	44	6.0	6.7
870324	12:49:48.9	37.4N	137.9E	39	5.7	5.4

Table 2
Epicentral distance (Δ) between seismic events and seismological stations of the study. θ is the angle between the arrival angle of the Rayleigh wave and the great circle that passes through the two stations

Event	Stat 1	Stat2	Δ1 (°)	Δ2 (°)	θ(°)
840211	NE03	NE02	18.8	20.0	32.2
850606	KONO	NRA0	65.5	67.0	1.8
851012	KONO	NRA0	66.1	67.6	2.4
851018	NRA0	KONO	72.4	73.8	2.0
860212	NRA0	KONO	74.8	76.3	1.5
860515	NE02	NE03	71.6	73.0	1.4
860517	NE02	NE03	71.6	73.0	1.4
861122	NRA0	KONO	76.1	77.6	0.5
861130	NRA0	KONO	72.8	74.3	3.2
870206a	NRA0	KONO	74.6	76.0	2.2
870206b	NRA0	KONO	74.5	76.0	2.2
870324	NRA0	KONO	72.9	74.3	0.5

to the profile. An event (840211) is included in the tables for which the Rayleigh waves arrive with a large angle (30°) relative to the profile NE02–NE03. Figs. 2 and 3 are examples of raw data that were selected for analysis (Fig. 2: event 860517, stations NE02 and NE03; Fig 3: event 861122, stations NRA0 and KONO).

3. Phase velocity analysis

3.1. Method

The phase velocity as a function of period was calculated by using the cross spectrum of the two filtered records, a classical method for measurements of time delays of almost identical signals (see, e.g., [23]). The phase velocity (c) is related to the phase ($\Delta\phi$) of the cross spectrum by:

$$c(\nu) = \Delta r 2\pi\nu/\Delta\phi(\nu) \quad (1)$$

where ν is the frequency and Δr the distance between the two stations.

Prior to the calculation of phase velocities, the records were band pass filtered between 10 and 200 s. Phase velocities were calculated for periods between 20 and 100 s with an interval of 10 s. For each period T, a time window was applied to the signals. Based on the group velocity dispersion

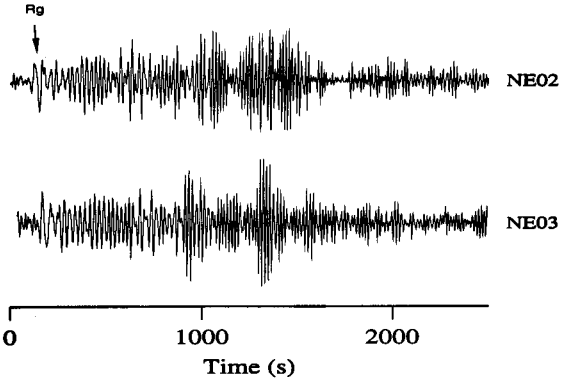

Fig. 2. Raw data for the vertical component at stations NE02 and NE03 for event 860517.

curves, the time window was centered on the arrival time of maximum energy of the surface wave at period T. The phase velocity was finally calculated using (1).

Application of a time window induces a smoothing of the spectra, with the length of the time window ($3T$ in the results presented here) controlling the degree of smoothing. Smoothing is known to stabilize the measurements of phase velocities (e.g., [24]) and is a currently used technique in surface wave studies.

The coherence as a function of frequency was calculated to estimate the quality of the phase velocity measurements (see, e.g., [23,25]). Only phase velocities that corresponded to frequency intervals where the coherence was stable and

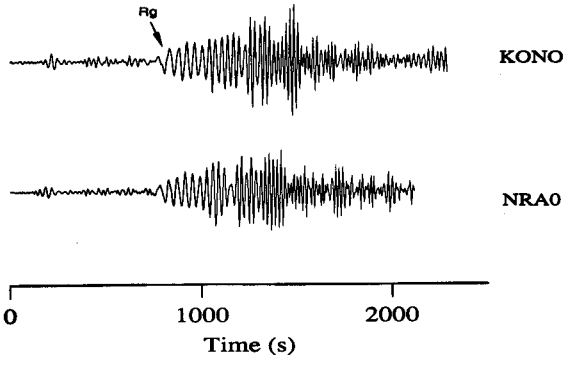

Fig. 3. Raw data for the vertical component at stations NRA0 and KONO for event 861122.

greater than 0.9 were retained. We furthermore verified that the length of the time window did not significantly influence the phase velocity measurements.

3.2. Results

For the Danish area, phase velocities were measured for Rayleigh waves of events 860515 and 860517. Fig. 4a shows these dispersion curves, which are very similar. The general shape of the curves shows a steep increase in phase velocities for periods between 20 and 40 s. The high phase velocity at the 40 s period was independent of the parameters used in the analysis and, as for the other periods, it was verified by group velocity analysis that there was no interference with other waves. For periods longer than 40 s, the phase velocities are almost constant 4.0–4.1 km/s. Fig. 4a also shows the dispersion curve for event 840211 for which the Rayleigh waves arrive with an angle of approximately 30° to the profile. The phase velocities for this event was measured between 30 and 70 s, due to low signal to noise ratio for periods over 70 s and interference between different waves at 20 s. The phase velocities of event 840211 has an almost constant offset towards higher velocities. At large angles between Rayleigh wave path and profile the phase velocity is very sensitive to the exact arrival angle and Fig. 4b shows that the offset can be explained by a deviation from the theoretical great-circle path of approximately 2.5°. The shape of the curve is very similar to those of events 860515 and 860517. For these two events, the phase velocities are not sensitive to the arrival angle of the Rayleigh waves because this angle is small relative to the profile between the two stations. The average phase velocities of events 860515 and 860517 are shown in Table 3 and Fig. 5 (solid line).

Table 3
Measured phase velocities (C) for Denmark and southern Norway

Period(s)	C Denmark (km/s)	C Norway (km/s)
20	3.44±0.003	3.68±0.03
30	3.86±0.02	3.89±0.06
40	4.10±0.003	3.95±0.04
50	4.03±0.02	3.93±0.06
60	4.03±0.03	4.03±0.06
70	4.07±0.03	4.08±0.13
80	4.08±0.03	4.17±0.13
90	$4.04^{\pm?}$	

KONO and NRA0 have different instrument responses which must be corrected for before calculating the phase velocities. Due to the very short distance between the two stations, even small errors in the correction for instrument response may lead to significant errors in the phase velocity measurements. Removal of instrument responses from data published on CD-rom for KONO and NRA0 did, in fact, lead to unrealistic phase velocities. An alternative to the use of

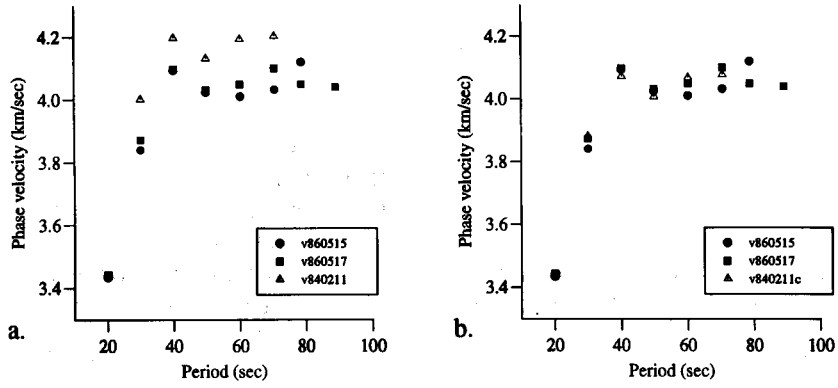

Fig. 4. Observed phase velocities for Denmark. (a) No correction applied for event 840211. (b) Correction equivalent of a 2.5° deviation from great-circle path applied to event 840211.

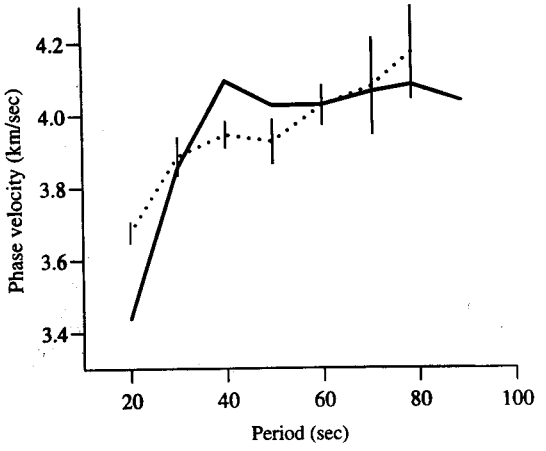

Fig. 5. Observed phase velocity dispersion curves. Solid line = Denmark; dotted line = Norway.

instrument-corrected records is to analyse signals from two events where the Rayleigh waves propagate through the stations on the same great circles but in opposite directions. The measured (ϕ_m) phase at each of the two stations is the sum of the phase (ϕ) of the signal and the phase ($\Delta\phi_i$) of the instrument response:

$$\phi_m = \phi + \Delta\phi_i \quad (2)$$

To eliminate the influence of the instrument response, the phase difference at a given frequency is calculated between the two stations for waves propagating from NRA0 to KONO and similarly for waves propagating from KONO to NRA0. The sum of these measured phase differences eliminates the phases of the instruments. Insertion of (1) in this sum of phase differences shows that the phase velocity, c, can be calculated by:

$$c = \frac{2c_1c_2}{c_1 + c_2} \quad (3)$$

where c_1 and c_2 are the apparent phase velocity of waves propagating in opposite directions through the two stations. This expression is valid for all frequencies.

Phase velocities were calculated separately for Rayleigh waves that had propagated along the profile from north to south between NRA0 and KONO and vice versa. For both directions, the agreement between dispersion curves of different events was good. This confirms that the two station responses had not evolved significantly with time and that expression (2) is valid for the events considered. The two average N–S and S–N dispersion curves were used to derive the dispersion curve for the area using Eq. (2). This curve is shown in Table 3 and Fig. 5 (dotted line). It shows a gradual increase in phase velocities from 3.7 to 4.2 km/s between periods of 20 and 90 s.

It is not straightforward to estimate the uncertainties related to the phase velocity measurements because the distance between the stations is very short. This means that small errors in the estimation of phase differences of the seismic signals induce large errors in the phase velocity measurements. A major problem in estimating uncertainties is the insufficient amount of data for a proper statistical analysis. The coherence between signals can be used to estimate the uncertainty of the measurements if the signals are assumed to contain only one wavetrain and additional non-correlated noise, an assumption which is not valid in the case of seismic signals. For short profiles, seismic arrivals due, for example, to multipathing effects can be coherently present on both records and systematic errors can be present. Error estimates based on uncertainties in source and station locations, for example, are small compared to these other effects. This is also true for errors due to deviations from the great circle path, where a simple polarization analysis of horizontal components showed that such deviations were less than 2°.

In spite of the small amount of data, we tentatively estimated the uncertainties of the two phase velocity curves in Fig. 5 by the difference between measured curves. For western Denmark, the two phase velocity curves are in good agreement, which implies small error bars. This estimate may be optimistic because the records can be systematically biased due to a same source location of the two earthquakes. On the other hand, analysis of the event with Rayleigh waves arriving with an angle of approximately 30° to the profile show the same general shape of dispersion curve event, although this event location and epicentral dis-

tance is very different to those of events 860515 and 860517.

For the dispersion curve from southeastern Norway, the procedure was the following: for the 7 events with surface waves propagating from north to south, the average curve and the standard deviation was calculated. For the 2 events with surface waves propagating from south to north, the average was calculated and the standard deviation was estimated as half the difference of the two curves. The final phase velocity curve for Norway was found by applying Eq. (2) on these two average curves and the error bars were found by applying (2) on the extreme values (average curves ± standard deviations). For these curves, no systematic bias due to earthquake locations is expected and the use of extreme values may imply that the errors in this case are overestimated.

There are two major differences between the phase velocity curves for western Denmark and southern Norway. First, the values of the dispersion curves are significantly different at the 40–50 s period. Secondly, the overall shape of the curves is different, with, for Denmark, a sharp increase in phase velocities between 20 and 40 s and an almost constant phase velocity at longer periods, while the curve for southern Norway increases regularly between 20 and 80 s. The agreement between different curves for the same path indicates that, in spite of the uncertainties in the measurements, these differences can be considered significant and that western Denmark and southern Norway belong to different tectonic units.

4. Inversion of dispersion curves

The dispersion curves of the phase velocity were inverted to obtain the shear wave velocity as a function of depth using computer programs published by Herrmann [26]. Due to the uncertainties in the measured phase velocities we did not attempt to find very detailed models, nor to estimate exact shear wave velocities in the crust and upper mantle. Instead, the inversions were performed to see how the difference between the two dispersion curves were related to differences in the lithospheric structure.

A one-dimensional, layered earth was assumed. The phase velocity is a non-linear function of the shear wave velocities so an iterative procedure was used where each iteration is a stochastic, damped, least-squares inversion of perturbations of the shear wave velocity in each layer. An a priori model was introduced for which the thickness of each layer and the elastic parameters, except the shear wave velocities, were kept constant during the inversion. For the dispersion curves shown in Fig. 5, this procedure gives a reasonable fit after only a few iterations between the observed dispersion curve and the model dispersion curve (dispersion curve of the final earth model).

The solution may depend on the a priori estimate of the shear wave velocities that we introduce in the inversion. This problem can be eliminated by the use of simple earth models. On the other hand, the choice of the layer thicknesses is critical when such simple models are used. Several test runs were therefore performed, with models containing up to 15 mantle layers, in order to detect depths where significant velocity changes appeared during the inversion. Neighbouring layers which, after a few iterations, were characterized by approximately the same shear wave velocity and resolution kernel were merged into one unit. No further simplifications of the model were made when the fit between the observed dispersion curve and the model dispersion curve started to decrease. A two-layer crustal model was used in which the thicknesses of upper and lower crust were based on results of deep seismic surveys. Even though the layer thickness is slightly different in the two sets of inversions, the starting velocity models of the mantle were similar, with slightly increasing shear and compressional wave velocities between the top of the mantle and the base of the model (300 km depth).

The crustal model for western Denmark was based on results of the EGT deep seismic surveys in the area [16]. In the area between NE02 and NE03, the Moho depth varies slightly around a value of 30 km. The thickness and structure of the upper crust varies considerably but this unit is

too shallow to influence the dispersion curve at periods longer than 20 s.

Fig. 6a shows a six-layer model of the lithosphere beneath Denmark that accounts for the general trends in the observed dispersion curve (Fig. 6b). The model is characterized by a low velocity layer that starts at a depth of about 110 km. The resolution of the shear wave velocity as a function of depth is shown for each layer to the right of the model. The shear wave velocities are well resolved for the first five layers, while the velocity in the deepest layer is poorly resolved. A series of inversions with different a priori models were performed to find the constraints on the upper and lower boundaries of the low velocity layer. The tests showed that the upper boundary of the low velocity layer must lie between a depth

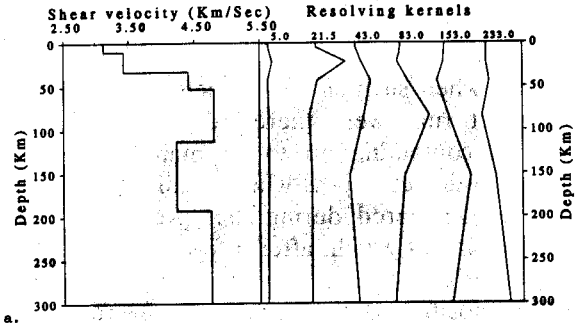

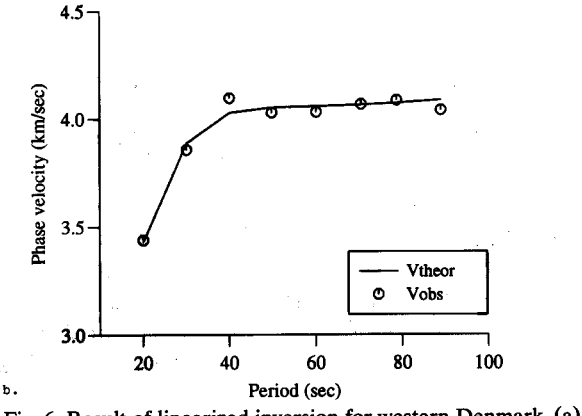

Fig. 6. Result of linearized inversion for western Denmark. (a) Velocity model and resolving kernels. (b) Fit between the observed dispersion curve (O) and the dispersion curve for the velocity model (line).

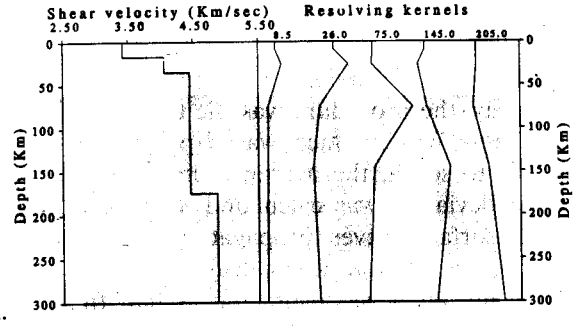

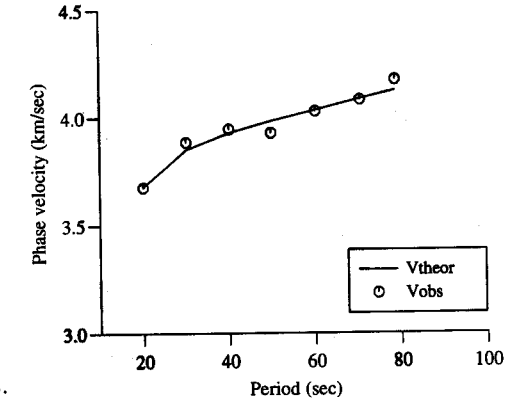

Fig. 7. Result of linearized inversion for south eastern Norway. (a) Velocity model and resolving kernels. (b) Fit between the observed dispersion curve (circles) and the dispersion curve for the velocity model (line).

of 90 and 130 km. This procedure also showed that it was not possible to find the depth of the lower boundary of the low velocity layer, except that the layer is at least 50–60 km thick.

Deep seismic data for southeastern Norway show Moho depths of about 35 km between NRA0 and KONO [27,28]. Thus, the a priori models used in the inversions included a 35 km thick, two-layer crust.

A five-layer model of shear wave velocities beneath southeastern Norway (Fig. 7a) is sufficient to model correctly the observed dispersion curve (Fig. 7b). Data can be explained by a model without a low velocity layer in the uppermost mantle but the data do not exclude the presence of a low velocity zone. However, such a zone must either be thin and compensated by a neighbouring high velocity layer or not have shear

wave velocities significantly lower than those of the surrounding layers. For the model presented in Fig. 7 the resolution is acceptable for depths down to 200 km.

For both models, it is necessary either to extend phase velocity measurements to longer periods or to analyse higher modes to find shear wave velocities in the mantle below 200 km. The use of short profiles and two-station measurements makes it difficult to measure phase velocities above 80–90 s correctly and, furthermore, the signal to noise ratios for the data were low above 100 s. Group velocity analysis did not reveal sufficiently stable higher modes to use them in a phase velocity analysis.

The stability of inversion results was verified by a number of test runs which included:

(1) inversions with dispersion curves in the period range 20–70, 20–80, and 20–90 s;
(2) inversions for southern Norway with the final model for Denmark (Fig. 6a) used as the starting model;
(3) inversions for Denmark with the final model for Norway (Fig. 7a) used as the starting model.

These verifications showed that the presence of a low velocity layer beneath Denmark is controlled by the general shape of the dispersion curve and not by the phase velocities at very long periods. It is, therefore, particularly the phase velocities at 40–50 s and the difference of slope at longer periods that discriminate between the two dispersion curves. To model the high phase velocity accurately for Denmark at 40 s it was necessary to replace the thick upper mantle layer by a pile of thinner layers but the resolution was very poor for such an inversion.

Although we cannot identify any details in crust/upper mantle structure from the observed dispersion curves, the inversions confirm that the lithospheric structure in the area changes significantly over a distance of only 400 km: western Denmark has a structure similar to that of western Europe and the North Sea area [9,13,19] and southeastern Norway has a predominantly shield-like crust/mantle structure with general characteristics similar to those proposed for the Baltic shield [9,14].

5. Conclusions

It is, in principle, possible to infer the upper mantle structure in small tectonic units from the analysis of surface waves recorded at closely spaced long period or broad-band stations. The analysis requires very high quality, digital data, which means that the sparse coverage of such long period and broad-band stations in most areas is a major obstacle to a more widespread analysis of surface waves along short profiles. Nevertheless, such analysis can constrain models found by surface wave studies for long profiles. More specifically, they can be used to detect whether a boundary that reaches the upper mantle is present between two tectonic units that are observed at the surface. This kind of independent information is useful for modeling other geophysical data, such as heat flow and refraction seismic data.

We found significant differences in dispersion curves of Rayleigh waves for southeastern Norway and western Denmark. These differences imply that the upper mantle structure of the two regions is different; changing from a structure with a pronounced LVZ to a structure with a weak or no LVZ. Western Denmark appears to belong to the west European Platform, while southeastern Norway has a shield-like mantle structure. We cannot distinguish if the change in the upper mantle structure is gradual or abrupt. Our results suggest, however, that the Sorgenfrei–Tornquist Zone coincides with — and may be the surface expression of — a major transition zone in the upper mantle.

Acknowledgements

We thank Søren Gregersen and Erik Hjortenberg for valuable discussions. Thanks also to Nils-Olov Bergquist, Hilmar Bungum, François Glangeaud, Jens Havskov, Bernt Hokland, Jerôme Mars, Ragnar Slunga and Lisbeth Engell Sørensen who have contributed to the project by discussion and help in obtaining data. [FA]

References

[1] R. Meissner, Th. Wever and E.R. Flüh, The Moho in Europa — Implications for crustal development, Ann. Geophys. 5, 357–364, 1987.

[2] J. Ansorge, D. Blundell and St. Mueller, Europe's lithosphere — seismic structure, in: A Continent Revealed: The European Geotraverse, D. Blundell, R. Freeman and St. Mueller, eds., pp. 33–69, Cambridge Univ. Press, Cambridge, 1992.

[3] V. Cermák and E. Hurtig, Heat flow map of Europe, in: Terrestrial Heat Flow in Europe, V. Cermák and and L. Rybach, eds., Springer, Berlin, 1979.

[4] E. Hurtig, V. Cermák, R. Haenel and V. Zui, eds., Geothermal Atlas of Europe, Herman Haack, Gotha, 1992.

[5] V. Cermák and L. Bodri, Three-dimensional deep temperature modelling along the European Geotraverse, Tectonophysics, in press.

[6] N. Balling, Heat flow and lithospheric temperature in the Baltic Shield — northern segment of the European Geotraverse, Tectonophysics, in press.

[7] G. Nolet, Upper mantle under western Europe inferred from the dispersion of Rayleigh waves, J. Geophys. 43, 265–285, 1977.

[8] G.F. Panza, St. Mueller, G. Calcagnile, The gross features of the lithosphere–asthenosphere system in Europe from seismic surface waves and body waves, Pure Appl. Geophys. 118, 1209–1213, 1980.

[9] G. Calcagnile, The lithosphere–astenosphere system in Fennoscandia, Tectonophysics 90, 19–35, 1982.

[10] St. Mueller and G.F. Panza, The lithosphere–asthenosphere system in Europe, In: D.A. Galson, St. Mueller and B. Munsch, eds., 1st EGT Workshop: The Northern Segment, pp. 23–26, European Science Foundation, Strasbourg, 1984.

[11] R. Snieder, Large-scale waveform inversions of surface waves for lateral heterogeneity 2. Application to surface waves in Europe and the Mediterranean, J. Geophys. Res. 93, 12067–12080, 1988.

[12] G. Calcagnile, P. Pierri, V. Del Gaudio and St. Mueller, A two-dimensional velocity model for the upper mantle beneath FENNOLORA from seismic surface waves and body waves, in: R. Freeman, P. Giese and St. Mueller, eds., The European Geotraverse: Integrative Studies, pp. 49–66, European Science Foundation, Strasbourg, 1990.

[13] B. Dost, Upper mantle structure under western Europe from fundamental and higher mode surface waves using the NARS array, Geophys. J. Int. 100, 131–151, 1990.

[14] G. Calcagnile, Deep structure of Fennoscandia from fundamental and higher mode dispersion of Rayleigh waves, Tectonophysics 195, 139–149, 1991.

[15] A. Zielhuis and G. Nolet, Shear wave velocity variations in the upper mantle beneath central Europe, Geophys. J. Int., in press.

[16] EUGENO-S Working Group, Crustal structure and tectonic evolution of the transition between the Baltic shield and the North German Caledonides (The EUGENO-S Project), Tectonophysics 150, 253–348, 1988.

[17] A. Berthelsen, From Precambrian to Variscan Europe, in: D. Blundell, R. Freeman and St. Mueller, eds., A Continent Revealed: The European Geotraverse, pp. 153–164, Cambridge Univ. Press, Cambridge, 1992.

[18] E.S. Husebye, J. Hovland, A. Christoffersson, K. Åkstrom, R. Slunga and C.-E. Lund, Tomographical mapping of the lithosphere and asthenosphere beneath southern Scandinavia and adjacent areas, Tectonophysics 128, 229–250, 1986.

[19] G.W. Stuart, The upper mantle structure of the North Sea region from Rayleigh wave dispersion, Geophys. J. R. Astron. Soc. 52, 367–382, 1978.

[20] B. Dost, Preliminary results from higher-mode surface-wave measurements in western Europe using the NARS array, Tectonophysics 128, 289–301, 1986.

[21] G. Nolet, Partitioned waveform inversion and two-dimensional structure under the network of autonomously recording seismographs, J. Geophys. Res. 95, 8499–8512, 1990.

[22] A. Dziewonski, S. Bloch and M. Landisman, A technique for the analysis of transient seismic signals, Bull. Seismol. Soc. Am. 59, 427–444, 1969.

[23] K. Aki and P.G. Richards, Quantitative Seismology — Theory and Methods, Freeman, San Francisco, Calif., 1980.

[24] L. Knopoff, S. Mueller and W.L. Pilant, Structure of the crust and upper mantle in the Alps from the phase velocity of Rayleigh waves, Bull. Seismol. Soc. Am. 56, 1009–1044, 1966.

[25] G. Poupinet, W.L. Ellsworth and J. Frechet, Monitoring velocity variations in the crust using earthquake doublets: an application to the Calaveras Fault, California, J. Geophys. Res. 89, 5719–5731, 1984.

[26] R.B. Herrmann, Computer Programs in Seismology, Saint Louis Univ., 1987.

[27] B.R. Cassel, S. Mykkelveit, R. Kanestrøm and E.S. Husebye, A North Sea–southern Norway seismic crustal profile, Geophys. J. R. Astron. Soc. 72, 733–753, 1983.

[28] J.J. Kinck, E.S. Husebye and C.-E. Lund, The South Scandinavian crust: Structural complexities from seismic reflection and refraction profiling, Tectonophysics 189, 117–133, 1991.